

# LEGIBILITY NOTICE

A major purpose of the Technical Information Center is to provide the broadest dissemination possible of information contained in DOE's Research and Development Reports to business, industry, the academic community, and federal, state and local governments.

Although a small portion of this report is not reproducible, it is being made available to expedite the availability of information on the research discussed herein.

Los Alamos National Laboratory is operated by the University of California for the United States Department of Energy under contract W-7405-ENG-36

TITLE: THE PLUTONIUM-OXYGEN PHASE DIAGRAM

AUTHOR(S): John M. Haschke  
NMT-5

RECEIVED  
NOV 0 1990

SUBMITTED TO: American Chemical Society Books Department  
To be published in the symposium volume, "50th Anniversary of the Discovery of Transuranium Elements," compiled from presentations at the 200th ACS Meeting, Washington, D.C., August 26-31, 1990.



By acceptance of this article the publisher recognizes that the U.S. Government retains a nonexclusive, royalty-free license to publish or reproduce the published form of this contribution or to allow others to do so for U.S. Government purposes.

The Los Alamos National Laboratory requests that the publisher identify this article as work performed under the auspices of the U.S. Department of Energy.

**Los Alamos** Los Alamos National Laboratory  
Los Alamos, New Mexico 87545

**MASTER**

FORM NO. 836-94  
51 MAR 20 2010

UNLIMITED

# THE PLUTONIUM-OXYGEN PHASE DIAGRAM

by

John M. Haschke  
Los Alamos National Laboratory  
Nuclear Materials Technology, MS E506  
Los Alamos, NM 87545  
Phone: (505)665-3342; FAX (505)667-7966

## ABSTRACT

Identification of products formed by the reaction of plutonium metal with liquid water at 23°C indicates that the plutonium-oxygen phase diagram is similar to the cerium-oxygen and praseodymium-oxygen diagrams. Quantitative measurements of H<sub>2</sub> formation and analytical data suggest that a sequence of hydrolysis reactions produces oxide hydrides of trivalent plutonium, Pu<sub>2</sub>O<sub>3</sub>, mixed-valent oxides and PuO<sub>2</sub>. The intermediate oxides are the n = 7,9,10 and 12 members of the Pu<sub>n</sub>O<sub>2n-2</sub> homologous series. Properties of the residue formed by thermal decomposition of the initial hydrolysis product, plutonium monoxide monohydrate (PuOH), are consistent with the formation of metastable plutonium monoxide. Crystal-chemical, thermodynamic, and kinetic factors are evaluated, but definitive assignment of the equilibrium Pu-O diagram is not possible.

---

## INTRODUCTION

In efforts to define the chemical properties of the transuranium elements, early workers frequently relied on the lanthanides to predict and model the behavior of the actinides (1, 2). Since cerium and praseodymium have relatively stable trivalent and tetravalent oxidation states, a close analogy was anticipated. The approach met with only limited success.

The general properties of the lanthanide and transuranium oxides are consistent, but not identical. As described in comprehensive reviews (3, 4), the principle oxide phases of Ce and Pr are isostructural with those of the transuranium elements. The sesquioxides ( $M_2O_3$ ) are dimorphic and crystallize as hexagonal ( $\beta$ - or A-type) and bcc ( $\alpha$ - or C-type) phases. The dioxides ( $MO_2$ ) have fcc ( $CaF_2$ -type) structures. The existence of trivalent and tetravalent hydroxides or hydrated oxides is reported, but only the  $UCl_3$ -type  $M(OH)_3$  phases of the lanthanides are well characterized (5). With the single exception of  $EuO$ , products identified by early workers as NaCl-type monoxides are apparently ternary phases such as oxide carbides and oxide nitrides. An important feature observed for Ce and Pr, but not for the transuranium elements, is the formation of stoichiometric mixed-valent oxides between the  $M_2O_3$  and  $MO_2$  compositions.

The reaction of plutonium metal with water has been investigated during the past decade. The initial objective of the study was to define the corrosion of plutonium by water with different impurity levels. The experimental methods were simple, but the results show a complex and unanticipated chemistry. Evaluation of the data suggests that the Pu-O system and the lanthanide-actinide analogy merit reexamination.

#### A COMPARISON OF PU WITH CE AND PR

To evaluate the merits of employing Ce-O and Pr-O as models for Pu-O, it is instructive to compare properties that might indicate if intermediate mixed-valent plutonium oxides are possible. Ionic radius is a primary crystal-chemical indicator of stability and structure of ionic solids. Values compiled by Shannon (6) show that the cationic radii of Ce and Pr bracket those of plutonium. The M(III) and M(IV) radii of Pr, Pu and Ce in six-fold coordination are 0.99, 1.00 and 1.01 Å and 0.85, 0.86, and 0.87 Å, respectively.

Thermodynamic properties are critical because differences in electronic structure and binding of the 4f and 5f elements may be

sufficient to preclude formation of intermediate oxides of Pu. Since equilibrium relationships of the oxides are determined by free-energy surfaces and tangential relationships in temperature-composition space, the necessary information is unavailable for Pu. However, the stabilities of mixed-valent oxides are in part reflected by the relative stabilities of the terminal  $M_2O_3$  and  $MO_2$  phases. If one terminal oxide is extremely stable relative to the other, formation of intermediate phases may not be observed. A qualitative comparison of the electrode potentials for the aqueous M(III)-M(IV) half reactions indicates that  $CeO_2$  is more stable relative to  $Ce_2O_3$  than  $PuO_2$  is to  $Pu_2O_3$ .

Quantitative indication of the relative stabilities of the terminal oxides of Ce, Pr and Pu is provided by the molar free energies for  $O_2$  oxidation of  $M_2O_3$  to two moles of  $MO_2$  at 298K. Whereas the  $\Delta G^\circ$  (298) values obtained from free energies of formation of the Pr and Ce oxides (3, 7) are -54 and -343 kJ/mol, respectively, that calculated from data for Pu (4, 8-10) ranges from -289 to -406 kJ/mol. The wide range of values for Pu reflects differences in the derived free energy of formation of bcc  $Pu_2O_3$ . Although this variation is in part due to the identification of a phase at  $PuO_{1.61}$  as  $\alpha$ - $Pu_2O_3$ , the thermodynamic properties of the cubic oxide are poorly defined. Despite the uncertainty, the results suggest that Pu and Ce are similar and that mixed oxides are to be anticipated for plutonium.

The metal-oxygen phase diagrams for Ce and Pr (3) in Figures 1 and 2 and that for Pu (4, 11) in Figure 3 differ. The presence of mixed-valent homologous series phases ( $M_nO_{2n-2}$ ) for the lanthanides distinguishes their diagrams from that for plutonium. As shown by the values of n in Figures 1 and 2, the n = 12 series member is observed for Pr, but not for Ce. Although the ionic radii and thermodynamic properties for Pu lie within the range bounded by Ce and Pr, intermediate phases are not observed for Pu or other transuranium elements. The composition of the high-temperature phase at  $PuO_{1.61}$  is near that for the n = 5 series member, but the lanthanide analogy is incomplete.

The general features of Pu-O are, however, remarkably similar to those of Ce-O and Pr-O if the homologous series phases are ignored. At compositions near O/M = 1.5 and at low temperatures, the equilibrium relationships of the hexagonal  $M_2O_3$  and bcc  $M_2O_{3+\delta}$  phases (dashed curves) are uncertain. At higher compositions and temperatures near 600°C, the miscibility gaps close with formation of extended solid solutions of fluorite-related  $MO_{2-x}$ .

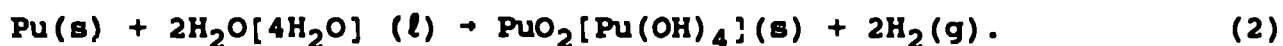
An important difference between the oxide systems of Ce and Pr and that of Pu is encountered in their oxidation kinetics. XRD (12) and XPS (13) data show that a surface layer of  $PuO_2$  forms on Pu metal during exposure to air or  $O_2$  at room temperature. This result is apparently accepted as a fact of actinide chemistry without regard for its kinetic implications. As shown in Figure 3,  $Pu_2O_3$ , not  $PuO_2$ , is the equilibrium oxide that coexists with metal. Equilibrium is achieved by heating  $PuO_2$ -coated metal to 150°C in vacuum (12, 13), but substoichiometric dioxide persists at temperatures up to at least 360°C under subatmospheric  $O_2$  pressures (14). XRD and XPS data for the oxide layer formed on Pu by reaction of low-pressure  $H_2O$  vapor at 120-250°C show a mixture of  $PuO_2$  and a second phase containing Pu(VI). The second phase is tentatively identified as  $Pu_3O_7$  (15). Like  $PuO_2$ , the new phase is a nonequilibrium product formed by a kinetically controlled reaction.

In contrast to the sluggish kinetics of Pu-O, the lanthanide oxides equilibrate readily with  $O_2$ . Redox reactions of intermediate oxides occur even in the absence of the large free energy gradient imposed by the presence of metal. The reactions are reversible and provide a convenient method for defining equilibria and thermodynamic properties at temperatures as low as 300°C (1). The origin of the kinetic differences between the lanthanides and plutonium is not understood, but may be important in interpreting the metal-oxygen phase diagrams.

## THE REACTION OF PLUTONIUM WITH WATER

### The Hydrolysis of Plutonium

Investigation of plutonium hydrolysis was initiated after unanticipated results were obtained in experiments designed to quantify the corrosion rate of Pu by tap water (16) and sea water (17) at room temperature. Information on the aqueous chemistry of plutonium (18) suggest that the corrosion should produce trivalent or tetravalent oxides or hydroxides according to Equation 1 or 2. Initial mass-loss



measurements yielded time-averaged corrosion rates and showed that fine black dioxide plus H<sub>2</sub> were produced (16). Subsequent pressure-volume-temperature (PVT) experiments provided dynamic rates from H<sub>2</sub> pressure-time curves, but failed to confirm the anticipated corrosion reactions (17). The observed ratio of hydrogen generated to metal consumed were near 0.6, not 1.5 or 2.0 as predicted by Equations 1 and 2. The corrosion process could not be described by either reaction.

The nature of the Pu+H<sub>2</sub>O reaction was studied in a series of PVT experiments (19). In neutral or weakly acidic solution, the corrosion rate R in mgPu/cm<sup>2</sup>h was found to vary with the molar anion concentration [X] (X = Cl<sup>-</sup>, NO<sub>3</sub><sup>-</sup>, SO<sub>4</sub><sup>2-</sup>, 10<sup>-7</sup>M < [X] > 2M) according to the relationship R = 15.90 [X]<sup>0.7</sup>. R is strongly pH-dependent and is immeasurably slow for pH > 8. PVT measurements showed that the H<sub>2</sub>:Pu ratio for complete reaction of the metal is 0.50. In an important PVT measurement, the continued evolution of H<sub>2</sub> was monitored for several hundred days after the metal had been consumed. These results are described in the following section.

## Results of Continued Hydrolysis

Insight into the chemistry of the Pu+H<sub>2</sub>O reaction at 23± 3 °C is provided by results of long-term measurements of H<sub>2</sub> generation (19). An 8.400 g sample of electrorefined Pu metal was submerged in 10 cm<sup>3</sup> of 1.0 M CaCl<sub>2</sub> solution contained in a glass-lined PVT apparatus with 94.93 cm<sup>3</sup> internal volume. The gas pressure in the system reached the 10 bar limit of the transducer after 100d and the pressure maintained at 8.5 ± 1.5 bar until day 270 by quantitative removal of gas. Thereafter, the pressure was confined to the 1.5 ± 0.5 bar range. The cumulative H<sub>2</sub>:Pu ratio was calculated as a function of time.

As shown in Figures 4 and 5, the H<sub>2</sub>:Pu ratio increases steadily as a function of time via a sequence of linear segments. H<sub>2</sub>:Pu ratios at the intersection points of the segments are indicated by numbers and horizontal arrows. The slope changes are extremely sharp except for the intersection near 1.75. The slopes in Figure 4 progressively decrease until zero slope (no reaction) occurs at 1.800 and 8.4 bar. As shown in Figure 5, H<sub>2</sub> generation resumes at a reduced pressure of 1-2 bar. Mass spectrometric analysis of gas samples obtained prior to the intersection at 2.00 show only H<sub>2</sub> while analyses of samples collected after that point show a mixture of H<sub>2</sub> and O<sub>2</sub>.

A conceptual framework is needed for interpreting the data. The PVT apparatus is a titration device that defines the extent of sample oxidation. The intersection points at 1.50 and 2.00 correspond to formation of trivalent and tetravalent products by processes like Equations 1 and 2. In a similar way the other intersection points correspond to the formation of solid products with specific hydrogen contents and plutonium oxidation states.

The conceptual frame work is derived in part from the properties of the H<sub>2</sub>:Pu-time curves. Except for the first segment, the linear correlation coefficients for the segments in Figures 1 and 2 are 0.999. This precise linearity suggests that the kinetics of all the hydrolysis reactions, except that of the metal, are controlled by the activities of two solid phases and

the equilibrium activities of species in solution. The reaction of metal is diffusion controlled by the product layer that subsequently spalls (16, 17), and the resulting parabolic time dependence gives rise to a lower (0.977) correlation coefficient. Within each segment, the hydrolysis rate is constant until the solid reactant is consumed. A slower constant rate is then established as the solid product from the preceding reaction is hydrolyzed. As with the assignments for 1.50 and 2.00, each intersection must be assignable to the formation of a rational chemical compound.

The complexity of assigning chemical reactions to the linear segments is increased by closely examining regions of the  $H_2$ :Pu-time curve. As shown in Figure 6, two additional segments and intersection points (1.714 and 1.778) are resolved by magnification of the region near 1.75. The existence of another intersection point at 1.833 is indicated by a similar evaluation of data for the 265-285 day time period in Figure 5. Since this linear segment appears immediately after the  $H_2$  pressure was decreased to 1 bar and is defined by only five data points, confidence in the existence of this slope change is less than those in Figures 4-6.

### Product Identification

Credible assignment of the reaction sequence for hydrolysis is contingent on at least partial identification of solid products. Essential information is provided by characterizing the solids present at  $H_2$ :Pu = 0.50 and 2.00 and by verifying that they are monophasic. Although six products are not identified, the reaction sequence is constrained to a reasonable set of reactions that must generate the initial product, account for the six intermediates and culminate in formation of the final product.

Samples (0.6-0.7 g) of the product at 0.50 were prepared in  $SiO_2$  microbalance containers by hydrolyzing the metal in 1 cm<sup>3</sup> of 0.01M NaCl solution in the PVT system. Reactions were terminated

at  $H_2:Pu = 0.50$  by drying the samples in dynamic vacuum. Hydrogen retention during evacuation was verified using quantitative gas expansion to dry representative samples. Microbalance data showed that traces of adsorbed water were removed in vacuum at  $70^\circ C$ .

The product formed at  $H_2:Pu = 0.50$  is identified as plutonium monoxide monohydride,  $PuOH$ . Mass gains measured during formation ( $6.9 \pm 0.2\%$ ) agree with the theoretical value (7.1%). XRD analysis of the black product show a single fcc ( $CaF_2$ -related) phase with  $a = 5.401(4)$  and an average particle size of 66 Å. Thermogravimetric analysis in vacuum shows that a 0.4% mass loss occurs over the  $105-195^\circ C$  range with evolution of  $H_2$ . XPS spectra of product layers on the metal indicate that oxygen is present as oxide, not as hydroxide. The results suggest that  $PuOH$  is an analog of the monoxide monohalides  $PuOX$  ( $X = F, Cl, Br, I$ ) (18).

The terminal product formed at  $H_2:Pu=2.00$  is  $PuO_2$ . XRD analysis of the vacuum-dried sample shows a single  $CaF_2$ -type phase with  $a = 5.404(3)$  Å. A mass loss of 3.4% occurring over the  $60-150^\circ C$  range during thermogravimetric analysis is attributed to water desorption and a constant mass over the  $150-500^\circ C$  range confirms the absence of hydroxide. The Pu content of the green product ( $87.1 \pm 1.1$  mass %) agrees with the theoretical value (88.19 mass%) and the lattice parameter of  $5.395(2)$  Å coincides with  $a = 5.397$  Å for  $PuO_2$ .

### Reaction Sequence

Assignment of the reaction sequence is readily achieved by defining the initial and final compositions in the conceptual framework as  $PuOH$  and  $PuO_2$ . Hydroxide does occur in the terminal phases and its presence in the intermediate products is doubtful. The experimental  $H_2:Pu$  values defined by the intersections of linear segments (19) are presented in Table 1 with the proposed sequence of eight hydrolysis reactions. The theoretical ratio

for each reaction is based on the cumulative sum of  $H_2$  for all reactions to that point. The agreement is remarkable.

The product assignment is consistent with the crystal chemistry anticipated of  $CeF_2$ -related phases. Examination of composition-structure relationships suggests how the hydrolysis process might occur. Whereas the fcc sublattice of metal ions is fixed at room temperature, anions such as  $O^{2-}$  and  $H^-$  are mobile and occupy the tetrahedral sites of the metal lattice in a 1:1 ratio at PuOH. Limited oxidation of PuOH according to the second reaction produces  $Pu_7O_9H_3$ , another oxide hydride of Pu(III). The phase is viewed as an altermvalent-anion analog of  $UY_6O_{12}$  in which the observed stoichiometry is achieved by substituting  $O^{2-}$  for 2/7 of the  $H^-$  sites in PuOH and forming an equal number of anion vacancies. Cubic  $Pu_2O_3$ , the  $n = 4$  member of the  $Pu_nO_{2n-2}$  homologous series, is derived by full replacement of  $H^-$  by  $O^{2-}$  and ordering of the anion vacancies in  $Ia\bar{3}$  symmetry within the  $Fm\bar{3}m$  metal sublattice.

Subsequent members of the oxide homologous series are formed by the anion altermvalency mechanism encountered with Ce and Pr (3). The  $n = 7, 9, 10$  and  $12$  series members are attained by progressive oxidation of Pu(III) to Pu(IV) and ordered occupation of vacant anion sites by oxygen. This process culminates in full site occupancy at  $PuO_2$ , the  $n = \infty$  series member.

Since the rates of the successive oxidation reactions in Table 1 are apparently controlled by equilibrium processes, kinetic effects typically encountered in heterogeneous systems must be absent. The possibility of rate control by dissociation of reacting species at the solid surface or by diffusion of species through a product layer is reduced by properties inherent to the system. Radiolytic dissociation of  $H_2O$  at the solid surface is promoted by 5.1 MeV  $\alpha$ -particles from  $Pu^{239}$  decay. The potential impact of diffusion is reduced by formation of extremely fine PuOH particles during the initial reaction.

## THE EXISTENCE OF PLUTONIUM MONOXIDE

Although XPS-AES spectroscopy shows that the surface phase previously identified as PuO is actually  $\text{PuO}_{0.6}\text{C}_{0.4}$ , and thermodynamic data suggest that the monoxide is unstable relative to Pu and  $\text{Pu}_2\text{O}_3$  (13), observations made during this study have reopened this question. Focus centers on the nature of the solid product formed by thermal decomposition of PuOH. Experimental evidence was obtained in the course of experiments designed to demonstrate that the monophasic fcc product ( $a = 5.401\text{\AA}$ ) identified as PuOH was not a mixture of fcc  $\text{PuO}_2$  ( $a = 5.397\text{\AA}$ ) and  $\text{PuH}_2$  ( $a = 5.360\text{\AA}$ ). Formation of this mixture seems remote because precisely half of the available hydrogen must form  $\text{PuH}_2$  while the remainder is liberated in the presence of unreacted Pu. The decomposition temperature of the product is  $250\text{--}350^\circ$  lower than the minimum dehydriding temperature observed for  $\text{PuH}_2$  (20), but a fine  $\text{PuH}_2$  powder might decompose more readily than anticipated. Since a diphasic product would dehydride to an oxide + metal mixture, rehydriding-dehydriding cycles were attempted to permit comparison of decomposition behavior.

Properties of the decomposition residue suggest that it is not a mixture of oxide and metal. The product is steel grey with a metallic luster and is unreactive to  $\text{H}_2$  at 0.13 bar and  $100^\circ\text{C}$  even though massive Pu readily reacts at these conditions. Microbalance data imply that an unpredictable chemical transformation occurs in the residue because it randomly becomes very reactive to  $\text{H}_2$  and residual gases temperatures in the  $220\text{--}435^\circ\text{C}$  range.

An impressive characteristic of the decomposition residue is its reactivity with oxygen. After one sample was found to be unreactive to  $\text{H}_2$  at  $100^\circ\text{C}$ , the microbalance system was evacuated and  $\text{O}_2$  was introduced as the sample cooled. The ensuing reaction initiated at low  $\text{O}_2$  pressure and was so violent and exothermic that the  $\text{SiO}_2$  container melted and fell from the support wire. XRD measurements were not attempted because of the extreme pyrophoric nature of the residue.

Properties of the residue from PuOH decomposition are consistent with those expected for metastable PuO. The metallic appearance and difference in reactivity toward oxidizing and reducing gases coincide with anticipated behavior of the monoxide. The sharp and unpredictable reactivity change observed during heating is consistent with nucleation of a disproportionation process that forms oxide and free metal.

### CONCLUSIONS

The oxide phases formed by hydrolysis of plutonium metal at room temperature are identical to those observed by praseodymium and imply that the lanthanide-actinide analogy for the transuranium elements is stronger than suggested by earlier results. Similar results for the transuranium hydrides are presented at this conference by Ward (21). In that case the analogy extends beyond phase relationships and structure type to include finer details such as anion ordering, magnetism and electronic structure.

The hydrolysis results lead to a substantially different Pu-O phase diagram than derived from high-temperature XRD measurement (11). The origin of the difference may well lie in the sluggish kinetics of the plutonium oxides. One might conclude that the mixed-valent oxides are stable, but the nucleation of intermediate phases is kinetically hindered. Likewise, the hydrolysis reactions described in this report are subject to kinetic constraints. The reaction times are long and equilibrium-like rate behavior is observed, but the sequence of fluorite-related products may not be the equilibrium phases. After the fcc arrangement is adopted by the metal atoms in PuOH, subsequent rearrangement to form equilibrium phases may be kinetically hindered. However, if the intermediate oxides are unstable, hydrolysis of CaF<sub>2</sub>-related Pu<sub>2</sub>O<sub>3</sub> should precede directly to CaF<sub>2</sub>-type PuO<sub>2</sub> by a single-step reaction. Although the validity of the phase diagram in Figure 3 seems doubtful, definitive conclusions cannot be drawn.

A severe impediment to the characterization of the  $\text{Pu}_2\text{O}_3$  seems to be the difficulty of sample preparation. The hexagonal phase is obtained only at extreme conditions the preparative procedure for cubic sesquioxide produces superstoichiometric  $\text{PuO}_{1.515}$  (2). The hydrolysis reaction apparently provides a novel and facile method for synthesis of cubic  $\text{Pu}_2\text{O}_3$ .

In addition to raising questions about plutonium-oxygen, the present observations suggest a broader range of concerns about the status of actinide chemistry. Plutonium monoxide monohydride is pyrophoric and is also formed by the reaction of the metal with water vapor (15); the properties and potential hazards are undefined. Further characterization of the oxide hydrides holds potential for addressing such issues and for defining the properties of hydridic residues formed during dissolution of actinide metals in mineral acid (22). Severe deficiencies in actinide and transuranium chemistry not only exist in new disciplines, but in areas that were studied years ago and are in need of reinvestigation.

#### ACKNOWLEDGEMENTS

This work was performed under auspices of the U.S. Department of Energy at the Rocky Flats Plant (Contract DE-4AC04-760P03533) and at the Los Alamos National Laboratory.

## REFERENCES

1. Asprey, L. B. "Equilibria in the Oxide Systems of Praseodymium and Americium," Ph.D. Thesis, 1949, University California, Berkeley.
2. Eyring, L. "Thermochemical Studies of the Oxides of Praseodymium and Americium and the Estimation of the Praseodymium (III)- Praseodymium (IV), Americium (III)-Americium (IV) Oxidation Potentials," Ph.D. Thesis, 1949, University of California, Berkeley.
3. Eyring, L. in Gschneidner, K. A., Jr.; Eyring, L., Eds., "Handbook on the Physics and Chemistry of Rare Earths," Vol. 3, Chap. 27, North Holland, 1979.
4. Colmenares, C.A. in McCaldin, J. O.; Somorjai, G., Eds., "Progress in Solid State Chemistry," Vol. 9, Chap. 5, Pergamon Press, 1975.
5. Brauer, G. Prog. Sci. Techn. Rare Earths, 1968, 3, 443.
6. Shannon, R. D. Acta Cryst., 1976, A32, 751.
7. Schumm, R. H.; Wagman, D. D.; Bailey, S.; Evans, W. H.; Parker, V. B. NBS Technical Note, 1973, 270-7.
8. Oetting, F. L. Chem. Rev., 1967, 67, 261.
9. Keller, C. in "Gmelin Handbuch der Anorganischen Chemie," Band 4, Teil C., Verlag Chemie GMBH, 1972.
10. Morss, L. R. in Katz, J. J.; Seaborg, G. T.; Morss, L. R., Eds., "The Chemistry of the Actinide Elements," Vol. 2, Chap. 17, Chapman Hall, 1986.
11. Gardner, E. R.; Markin, T. L.; Street, R. S., J. Inorg. Nucl. Chem., 1965, 27, 541.
12. Terada, K.; Meisel, R. L.; Dringman, M. R. J. Nucl. Mater., 1969, 30, 340.
13. Larson, D. T.; Haschke, J. M. Inorg. Chem., 1981, 20, 1945.
14. Stakebake, J. L.; Lewis, L. A. J. Less-Common Metals, 1988, 136, 349.
15. Stakebake, J. L. personal communication, EG&G Rocky Flats, Golden, CO, 1990.
16. Hodges, A. E., III; Reynolds, J. J.; Haschke, J. M. USDOE Report RFP-2891, Rockwell International, Golden, CO, 1979.

17. Hodges, A. E., III; Haschke, J. M. USDOE Report RFP-2919, Rockwell International, Golden, CO, 1979.
18. Cleveland, J. M. "The Chemistry of Plutonium," Chap. 9, Gordon and Breach, 1970.
19. Haschke, J. M.; Hodges, A. E., III; Bixby, G. E.; Lucas, R. L. USDOE Report RFP-3416, Rockwell International, Golden, CO, 1983.
20. Haschke, J. M.; Stakebake, J. L. in McCarthy, G. J, Rhyne, J. J.; Silber, H. B., Eds., "The Rare Earths in Modern Science and Technology," Vol. 2, Plenum, 1980; p. 577.
21. Ward, J. W. proceedings of this conference, 1990.
22. Katzin, L. I., J. Amer. Chem. Soc., 1958, 80, 5908.

#### DISCLAIMER

*This report was prepared as an account of work sponsored by an agency of the United States Government. Neither the United States Government nor any agency thereof, nor any of their employees, makes any warranty, express or implied, or assumes any legal liability or responsibility for the accuracy, completeness or usefulness of any information, apparatus, product, or process disclosed, or represents that its use would not infringe privately owned rights. Reference herein to any specific commercial product, process, or service by trade name, trademark, manufacturer, or otherwise does not necessarily constitute or imply its endorsement, recommendation, or favoring by the United States Government or any agency thereof. The views and opinions of authors expressed herein do not necessarily state or reflect those of the United States Government or any agency thereof.*

Table 1. Proposed sequence of hydrolysis reactions for plutonium at 23°C.

Hydrolysis Reaction	Cumulative H <sub>2</sub> :Pu Ratio	
	Theor.	Exptl. <sup>a</sup>
$\text{Pu} + \text{H}_2\text{O} \rightarrow \text{PuOH} + 1/2\text{H}_2$	0.500	0.507 (6)
$\text{PuOH} + 2/7 \text{H}_2\text{O} \rightarrow 1/7 \text{Pu}_7\text{O}_9\text{H}_3 + 4/7 \text{H}_2$	1.071	1.078 (23)
$1/7 \text{Pu}_7\text{O}_9\text{H}_3 + 3/14 \text{H}_2\text{O} \rightarrow 1/2 \text{Pu}_2\text{O}_3 + 3/7 \text{H}_2$	1.500	1.455 (38)
$1/2 \text{Pu}_2\text{O}_3 + 3/14 \text{H}_2\text{O} \rightarrow 1/7 \text{Pu}_7\text{O}_{12} + 3/14 \text{H}_2$	1.714	1.716 (170)
$1/7 \text{Pu}_7\text{O}_{12} + 4/63 \text{H}_2\text{O} \rightarrow 1/9 \text{Pu}_9\text{O}_{16} + 4/63 \text{H}_2$	1.778	1.763 (118)
$1/9 \text{Pu}_9\text{O}_{16} + 1/45 \text{H}_2\text{O} \rightarrow 1/10 \text{Pu}_{10}\text{O}_{18} + 1/45 \text{H}_2$	1.800	1.803 (2)
$1/10 \text{Pu}_{10}\text{O}_{18} + 1/30 \text{H}_2\text{O} \rightarrow 1/12 \text{Pu}_{12}\text{O}_{22} + 1/30 \text{H}_2$	1.833	1.831 (181)
$1/12 \text{Pu}_{12}\text{O}_{22} + 1/6 \text{H}_2\text{O} \rightarrow \text{PuO}_2 + 1/6 \text{H}_2$	2.000	1.993 (16)

<sup>a</sup>Uncertainties in the last digits are given in parenthesis.

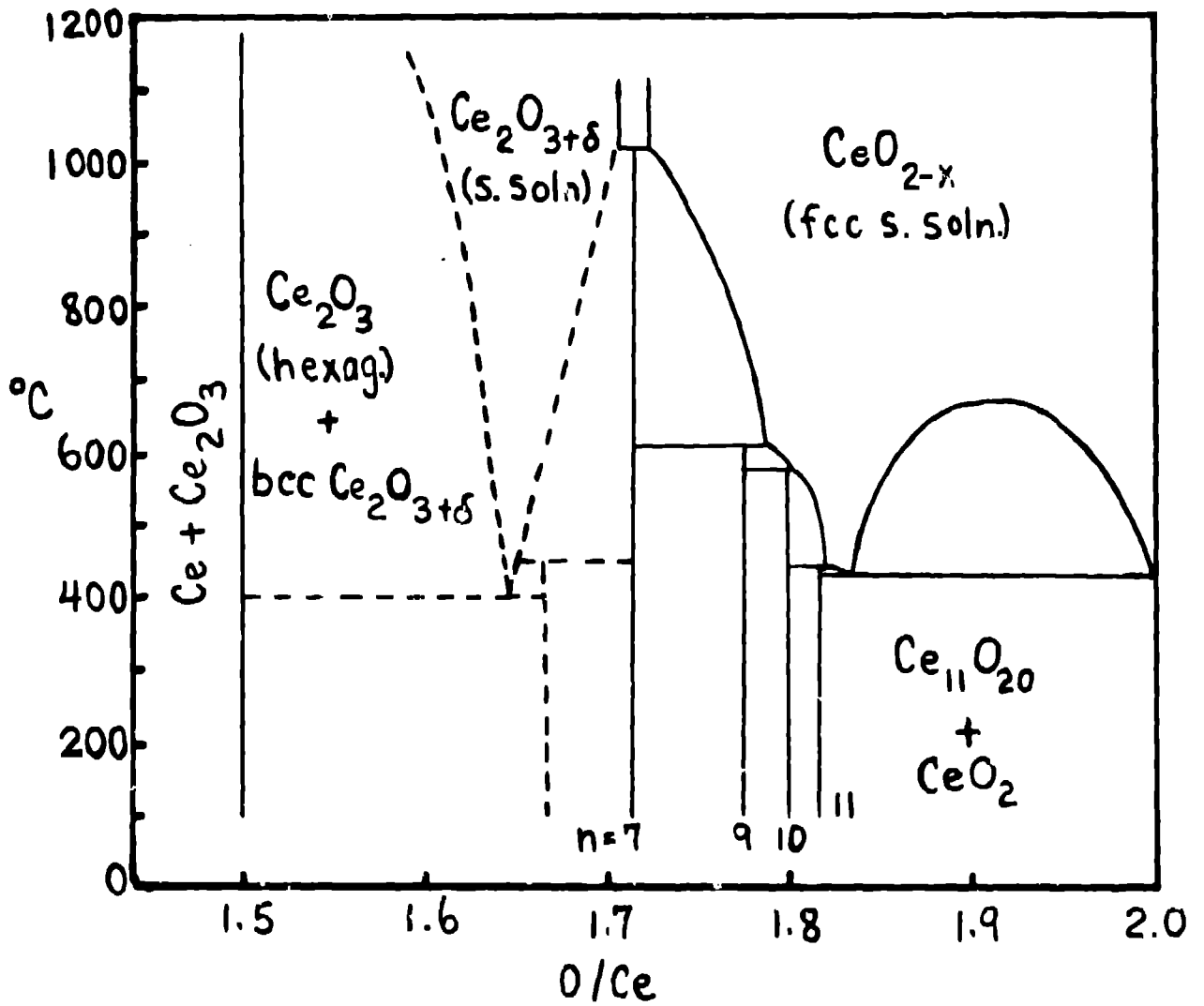


Figure 1. The idealized cerium-oxygen phase diagram (3).

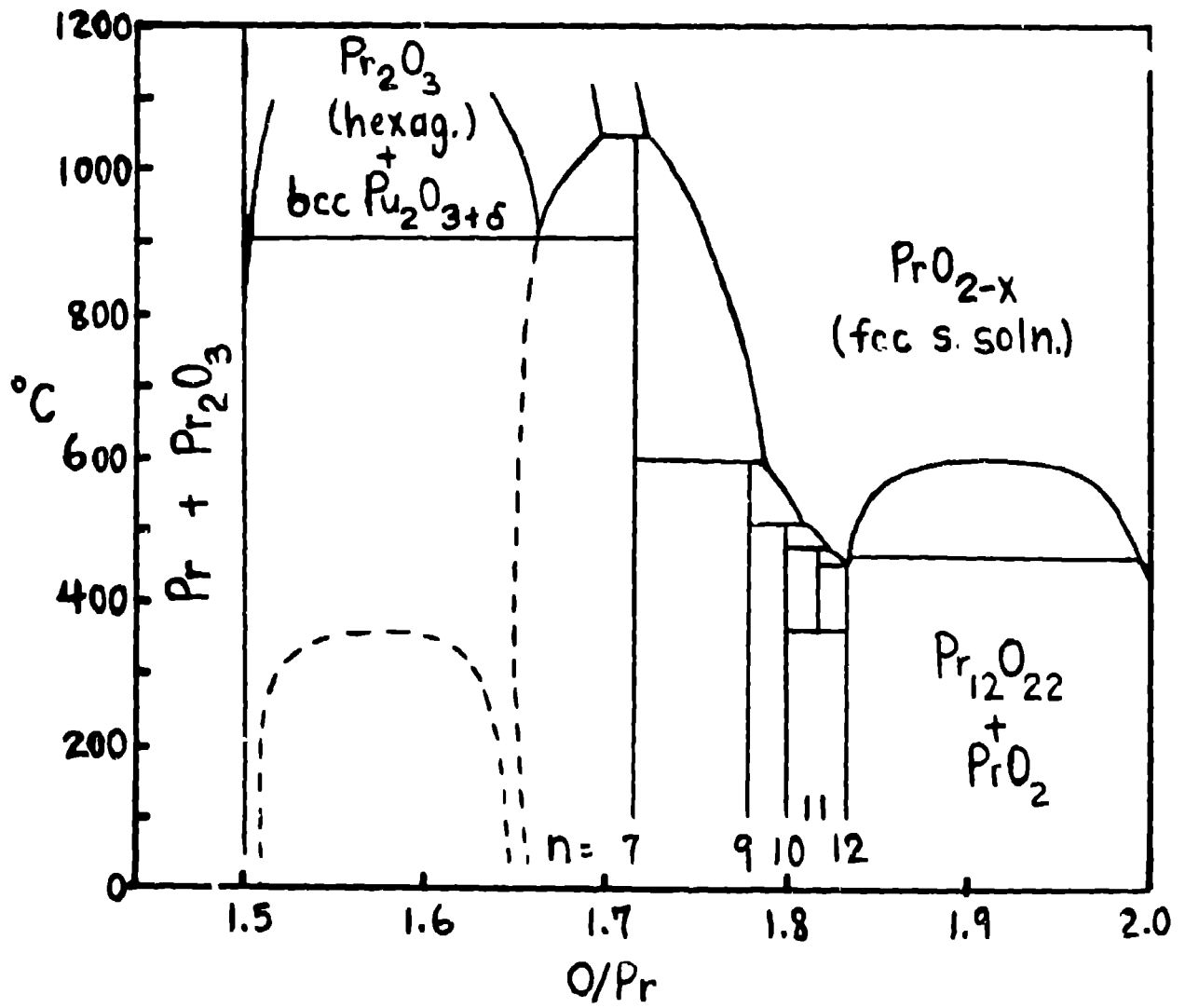


Figure 2. The idealized praseodymium-oxygen phase diagram (3).

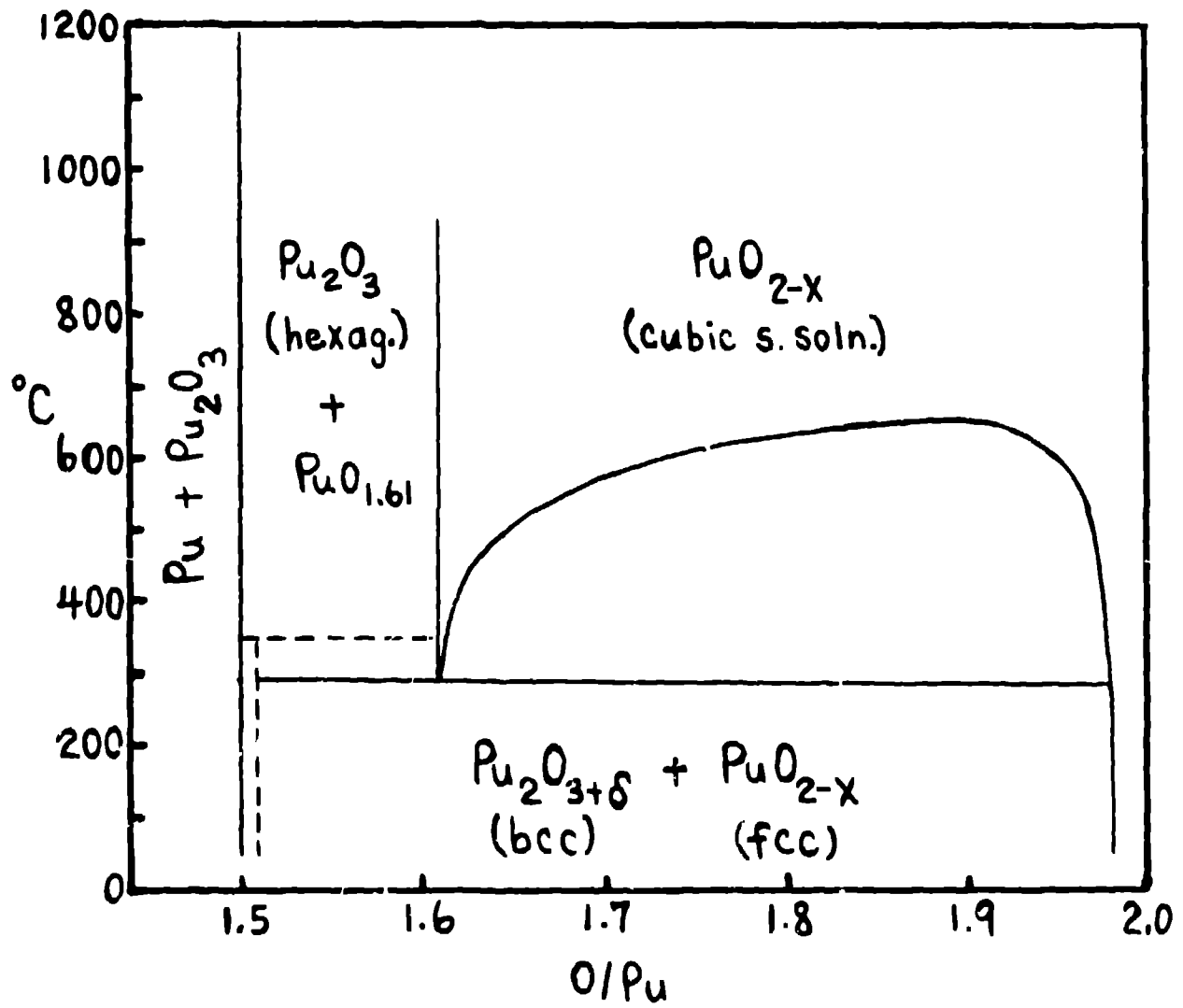


Figure 3. The plutonium-oxygen diagram (4, 11).

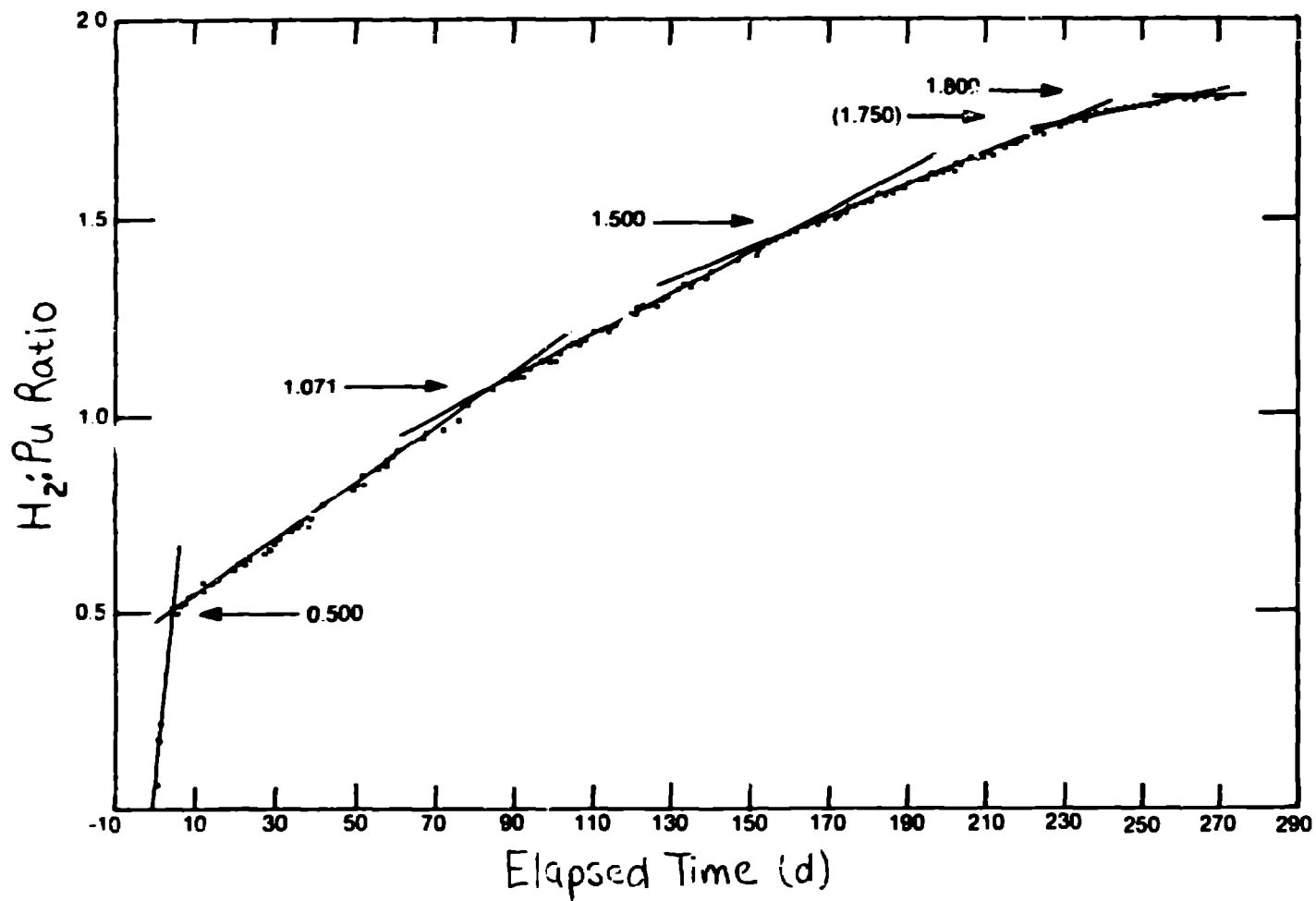


Figure 4. The time dependence of the H<sub>2</sub>:Pu ratio for the reaction of 1M CaCl<sub>2</sub> solution at 23°C and H<sub>2</sub> overpressures up to 10 bar.

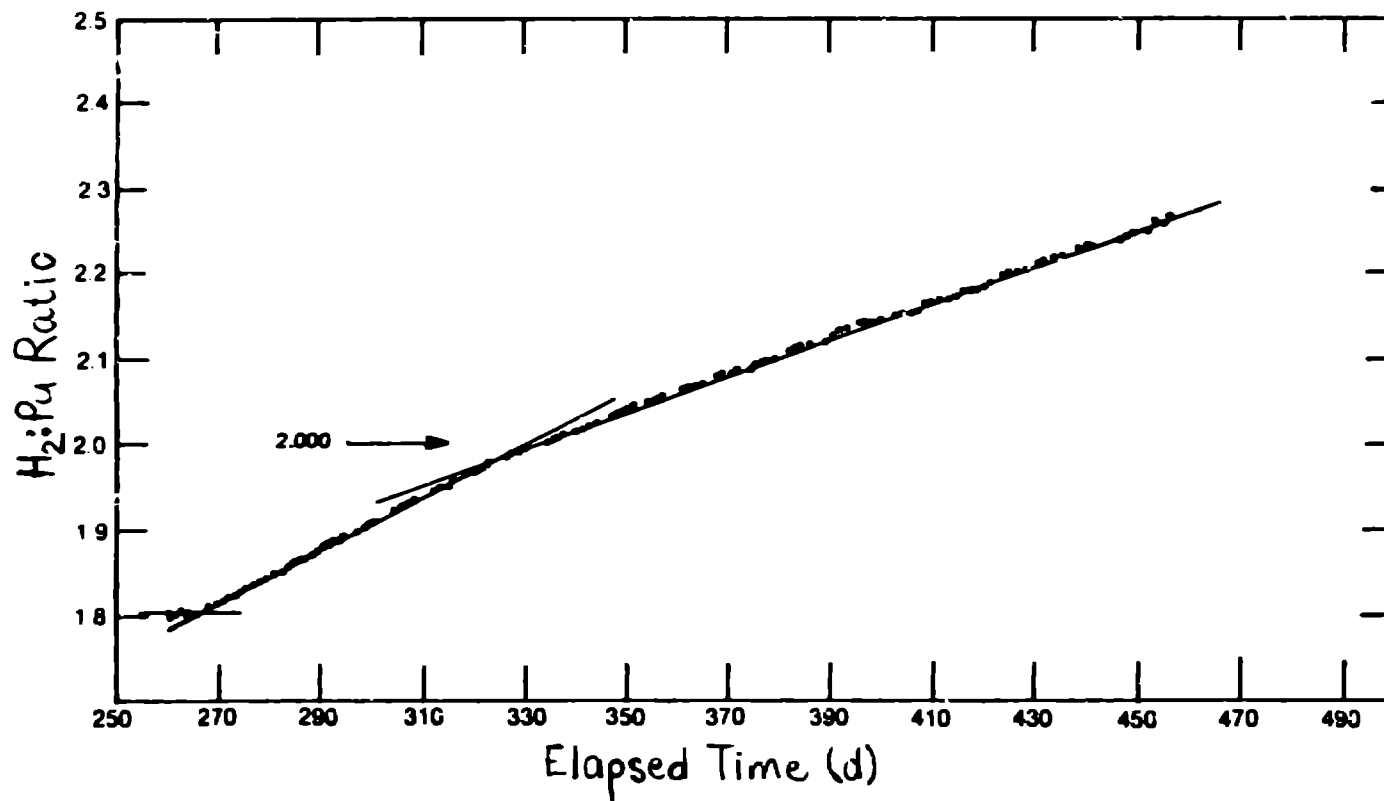


Figure 5. The time dependence of the H<sub>2</sub>:Pu ratio for the reaction of 1M CaCl<sub>2</sub> solution at 23°C and H<sub>2</sub> overpressures of 1.5 ± 0.5 bar.

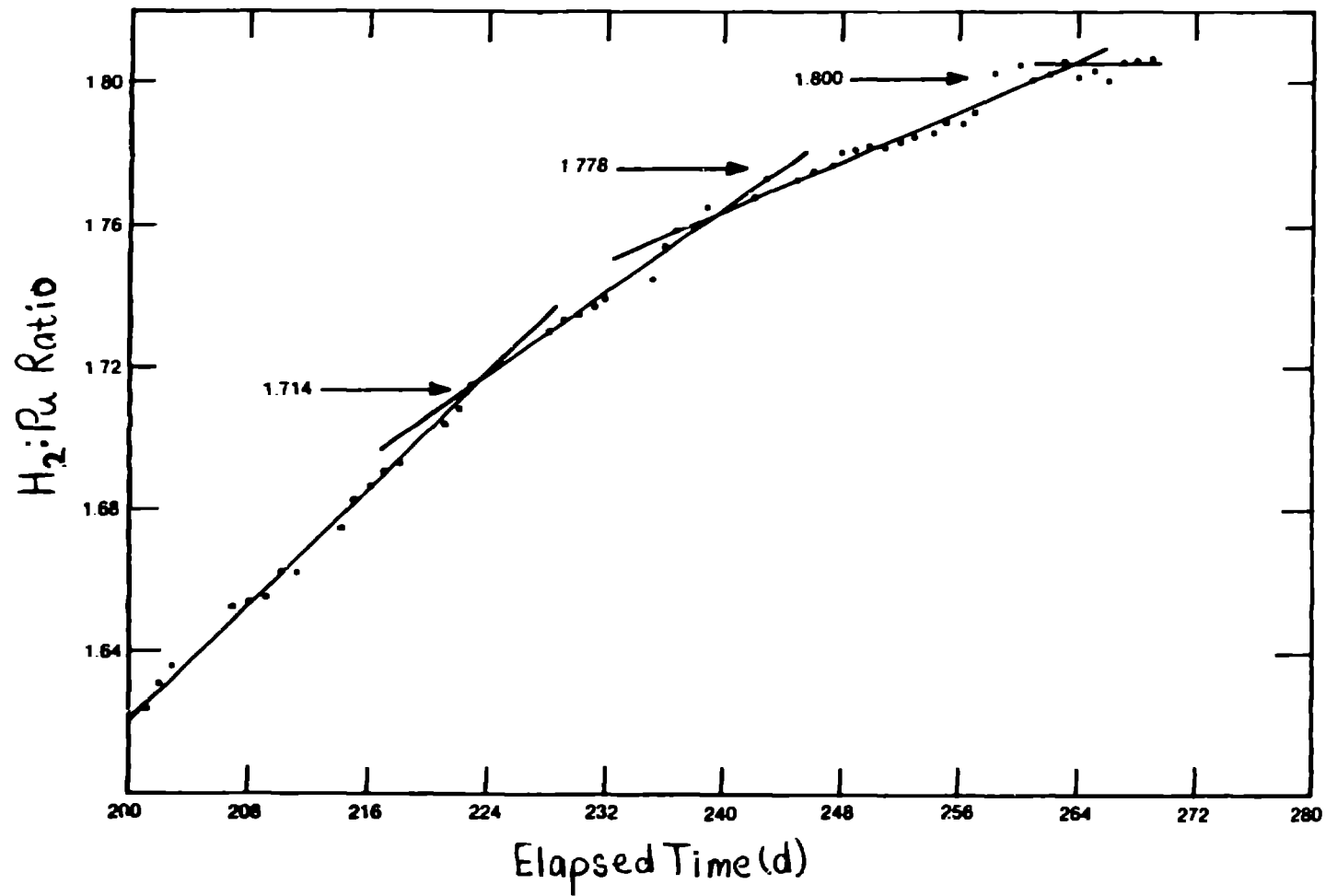


Figure 6. The time dependence of the H<sub>2</sub>:Pu ratio for the intersection near 1.75.